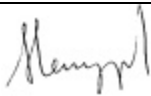# Final technical report
To Partner Project Agreement # 2006 p
Between the International Science and Technological Center, Design and Technological Institute of
Monocrystals SB RAS and the European Office of Aerospace Research and Development
(Beginning: 01.02.2001 Ending 01.02.2002)
Report Sent 12 February 2002

1. <u>Project Title:</u> **Performing of new nonlinear LiInS2 and LiInSe$_2$ crystals for estimation of their application outlooks**

2. Participating, Contracting Institutions

Name: Design @ Technological Institute of Monocrystals SB RAS		
Address:	**Street:** 43, Russkaya str.	**City:** Novosibirsk
Region:	Country: RUSSIA	Zip Code: 630058
Name of Signature Authority: Chepurov A.I.		
Tel: **+7 (3832)33-22-39**	Fax: **+7 (3832) 33-38-43**	E-mail: lisa@lea.nsk.su
Governmental Agency: Russian Academy of Sciences		

3. <u>Project Manager</u>

Name: **Isaenko Ludmila Ivanovna**		
Address:	**Street:** 5A, Vakhtangova str	**City:** Novosibirsk
Region:	Country: RUSSIA	Zip Code: 630058
Tel: **+7 (3832) 33-38-43**	Fax: **+7 (3832) 33-38-43**	E-mail: lisa@lea.nsk.su

4. <u>Foreign Partner</u>

Name: European Office of Aerospace Research and Development (EOARD)		
Address:	**Street:** 223-231 Old Marylebone Road	**City:** London
Region/State:	Country: England	Zip Code: NW1 5TH
Name of Signature Authority: Barbara A. Murphy		
Tel: **+44-(0)20-7514-4950**	Fax: **+44-(0)20-7514-4960**	E-mail:
Name of Contact Person: C. Martin Stickley, R.Reed		
Tel: **+44 171 514 4354**	Fax: **+44 171 514 4960**	E-mail: martin.stickley@london.af.mil ron.reed@london.af.mil

Report Documentation Page

Report Date 12022002	Report Type Final	Dates Covered (from... to) -

Title and Subtitle Performing Of New Nonlinear Liins2 And Liinse2 Crystals For Estimation Of Their Application Outlooks	**Contract Number**
	Grant Number
	Program Element Number
Author(s) Issaenko, Lioudmila	**Project Number**
	Task Number
	Work Unit Number
Performing Organization Name(s) and Address(es) Design and Technological Institute of Monocrystals 43 Russkaya str., Novosibirsk 630058 Russia	**Performing Organization Report Number**
Sponsoring/Monitoring Agency Name(s) and Address(es) EOARD PSC 802 BOX 14 FPO 09499-0200	**Sponsor/Monitor's Acronym(s)**
	Sponsor/Monitor's Report Number(s)

Distribution/Availability Statement
Approved for public release, distribution unlimited

Supplementary Notes

Abstract
This report results from a contract tasking Design and Technological Institute of Monocrystals as follows: The goal of project is to grow bulk LiInS2 crystals and to prepare batches of both LiInS2 and LiInSe2 crystals of selected forms such as oriented plates, parallelograms, and prisms for detailed study in the USA of the main properties such as their transparency, residual absorption due to deep levels, refractive indices and electric conductivity. The LiInS2 and LiInSe2 crystals will be characterised in chemical composition, crystal lattice parameters and energy gap, and compared with literature data. The as-grown crystals will be annealed in certain atmospheres for correction of their chemical composition, if necessary. Their optical quality will be tested using optical microscopy, shadow and interference techniques. Their further investigation in the U.S.A. is expected to allow an estimate of their future applications.

Subject Terms

Report Classification unclassified	**Classification of this page** unclassified
Classification of Abstract unclassified	**Limitation of Abstract** UU

Number of Pages
28

REPORT DOCUMENTATION PAGE

Form Approved OMB No. 0704-0188

1. AGENCY USE ONLY (Leave blank)	2. REPORT DATE	3. REPORT TYPE AND DATES COVERED
	12 February 2002	Final Report

4. TITLE AND SUBTITLE

Performing Of New Nonlinear Liins2 And Liinse2 Crystals For Estimation Of Their Application Outlooks

5. FUNDING NUMBERS

ISTC Registration No: 2006

6. AUTHOR(S)

Professor Lioudmila Issaenko

7. PERFORMING ORGANIZATION NAME(S) AND ADDRESS(ES)

Design and Technological Institute of Monocrystals
43 Russkaya str.,
Novosibirsk 630058
Russia

8. PERFORMING ORGANIZATION REPORT NUMBER

N/A

9. SPONSORING/MONITORING AGENCY NAME(S) AND ADDRESS(ES)

EOARD
PSC 802 BOX 14
FPO 09499-0200

10. SPONSORING/MONITORING AGENCY REPORT NUMBER

ISTC 00-7025

11. SUPPLEMENTARY NOTES

12a. DISTRIBUTION/AVAILABILITY STATEMENT

Approved for public release; distribution is unlimited.

12b. DISTRIBUTION CODE

A

13. ABSTRACT (Maximum 200 words)

This report results from a contract tasking Design and Technological Institute of Monocrystals as follows: The goal of project is to grow bulk LiInS2 crystals and to prepare batches of both LiInS2 and LiInSe2 crystals of selected forms such as oriented plates, parallelograms, and prisms for detailed study in the USA of the main properties such as their transparency, residual absorption due to deep levels, refractive indices and electric conductivity. The LiInS2 and LiInSe2 crystals will be characterised in chemical composition, crystal lattice parameters and energy gap, and compared with literature data. The as-grown crystals will be annealed in certain atmospheres for correction of their chemical composition, if necessary. Their optical quality will be tested using optical microscopy, shadow and interference techniques. Their further investigation in the U.S.A. is expected to allow an estimate of their future applications.

14. SUBJECT TERMS

EOARD, Physics, Solid State Physics

15. NUMBER OF PAGES

22

16. PRICE CODE
N/A

17. SECURITY CLASSIFICATION OF REPORT	18. SECURITY CLASSIFICATION OF THIS PAGE	19. SECURITY CLASSIFICATION OF ABSTRACT	20. LIMITATION OF ABSTRACT
UNCLASSIFIED	UNCLASSIFIED	UNCLASSIFIED	UL

NSN 7540-01-280-5500

Standard Form 298 (Rev. 2-89)
Prescribed by ANSI Std. 239-18
298-102

Technology Area: Solid State Physics
Category of Technology Development: Basic and Applied Sciences

5. Scope of activities:
Task 1. Purification of initial reagents, study of conditions of stable crystallization for LiInS$_2$ and LiInSe$_2$ of stoichiometric composition
Task 2. Study of thermal treatment effect on optical properties of LiInS$_2$ and LiInSe$_2$. Obtaining of bulk crystal. Refinement of crystal structure, determination of band gap width and type of transitions, responsible for the latter.
Task 3. Study of real structure, visualization of extended defects, optical spectroscopy study in the transparency range on rectangular pieces of LiInS$_2$ and LiInSe$_2$. Performing of characterized optical elements as plates and prisms from them for further investigation in Labs of Partner (EOARD).
Task 4. Preparing papers, reports about quality of crystals for Partner and for International meetings.

Works on Tasks 1-3 are carried out in full volume for LiInS$_2$ during 1-2 quarters and for LiInSe$_2$ during 3-4 quarters. Optical elements for Partner are performed from pieces, characterized in detail, and delivered in quarters 1-2 for LiInS$_2$ and in quarters 3-4 for LiInSe$_2$. The work in the Partners's Labs is carried out after receiving samples from DTIM.

Schedule of DTIM delivery of optical elements to Partner:
Quarter 1. 9 polished plates 6 x 6 x 1 mm^3 in size of LiInS$_2$ for three groups of measurements: residual absorption, electrical measurements and deep level spectroscopy);
Quarter 2. The LiInS$_2$ prisms with different orientation and 30° apex angle for refractive index measurements for three polarizations;
Quarter 3. 9 polished plates 6 x 6 x 1 mm^3 in size of LiInSe$_2$ for three groups of measurements: residual absorption, electrical measurements and deep level spectroscopy);
Quarter 4. The LiInSe$_2$ prisms with different orientation and 30° apex angle for refractive index measurements for three polarizations.

The goal of present proposal is to obtain bulk NLO LiInS$_2$ and LiInSe$_2$ crystals of optical quality, which are characterized in composition and structure using chemical, X-ray structural and optical methods as well as to perform optical elements for estimation of LiInS$_2$/LiInSe$_2$ outlooks for nonlinear optics.

6   EXPECTED RESULTS AND THEIR APPLICATITION

- The stability fields for $LiInS_2$ and $LiInSe_2$ will be established and bulk single crystals of high optical quality will be obtained.
- The identity of crystal structure for samples obtained in different conditions will be confirmed using the X-ray single crystal structural analysis, band gap width values and types of the transitions responsible for the latter;
- Real structure for obtained $LiInS_2$ and $LiInSe_2$ crystals will be studied, the main types of point and extended defects revealed and their formation conditions established.
- A samples of $LiInS_2$ and $LiInSe_2$ optical elements, characterized in composition, structure, optical properties, will be forwarded to Partner (EOARD) for determination of their most important physical parameters and estimation of their outlooks for nonlinear optics.
- The present proposal provides an element base for development of new laser devices, which are necessary to solve different analytical, ecological, medical and other problems in national and international scale.
- The results will be published in scientific journals and submitted on the international meetings.

7.1 MOTIVATION

Only few suitable nonlinear crystals are available for generation of coherent radiation tunable in the mid-IR (3 to 20 µm), a spectral region of great importance for vibrational molecular spectroscopy and atmospheric sensing. An active search for new nonlinear crystals for this region is in progress now. The new materials that can be successfully added to this limited list of crystals are $LiInS_2$ and $LiInSe_2$ (further LIS, LISe, respectively). The first one was first studied by Boyd and co-workers in the 70-ies [1], and has recently enjoyed renewed interest because of its attractive optical properties, such as the large transparency range from 0.35 to 13 µm and the high (estimated at 10.6 µm [1]) nonlinear susceptibility d_{33}=15.8 pm/V. No information about the nonlinearity of LISe was available, but it was expected to be higher. The main properties of $LiInS_2$ and $LiInSe_2$ crystals are given in Table 1.

One can see, that there are several additional advantages, which make the Li-based crystals very attractive for nonlinear optics:

- Increased thermal conductivity (lighter Li ion leads to an increase in lattice phonon frequencies and the Debye temperature): thermal conductivity of $LiInS_2$ is 5 times higher than that of $AgGaS_2$;
- Largest energy gap (3.59 eV at 300 K) among mid-IR crystals and as a result of this reduced effect of two-phonon absorption: for 800 nm the latter is two orders of magnitude lower than in $AgGaS_2$ crystals;
- Wurtzite-type lattice which is less prone to stresses and laminar defects (no sign anisotropy in thermal expansion coefficients); formation of solid solutions and doping for adjustment of phase-matching conditions are allowed [9].
- $LiInS_2$ and isotypes crystallize in the *mm2* point group, like KTP, and are pyroelectric. If $LiInS_2$ and $LiInSe_2$ have ferroelectric properties it could be a promising material for periodic poling and quasi-phase matching (QPM) but this question is still open.

Table 1. The main parameters of LiInS$_2$ crystals

Transparency range (μm)	0.35 – 13
Second order nonlinear susceptibility, d (pm/V)	d_{33} =15.8 [1]
	d_{31} = 8.35 ±1.7 [this work]
	d_{32} = 8.30 ±1.6 [this work]
Symmetry, point group	Orthorhombic, **mm2**
Lattice parameters, (A)	**a** = 6.894 [1] **a** = 6.878 [2]
	b = 8.064 **b** = 8.033
	c = 6.485 **c** = 6.462
Density (g/cm^3)	3.54
Melting point (ºC)	1000
Linear thermal expansion coefficients $a = 1/l*dl/dT$ at 300 K (K^{-1}) T is measured in °C	$a_x = (1.44 \times 10^{-8}\,T + 1.61 \times 10^{-5})$ [3]
	$a_y = (0.72 \times 10^{-8}\,T + 0.89 \times 10^{-5})$
	$a_z = (0.93 \times 10^{-8}\,T + 0.66 \times 10^{-5})$
Refractive indices, at 0.7μm	$n_x = 2.171$, $n_y = 2.212$, $n_z = 2.22$ [1]
at 10 μm	$n_x = 2.023$, $n_y = 2.059$, $n_z = 2.062$ [1]
Birefringence at 0.7-12 μm	0.01– 0.04
Birefringence change versus temperature at 300 K, $d(?n)/dT$, (1/°C)	$11.95 * 10^{-6}$ (along X) [4]
	$0.68 * 10^{-6}$ (Y)
	$12.72 * 10^{-6}$ (Z)
Energy gap (eV)	3.73 (80 K), 3.59 (300 K) [5]
Pyroelectric coefficient at 300 K (μC/m^2 K)	2.6 [6]
Bulk optical damage threshold at 5 μm , 500 fs pulses with 25 MHz repetition (GW/ cm^2)	> 6 [7]
Surface optical damage threshold at 800 nm, 200 fs, 1 kHz (GW/cm^2)	>140 [8]
Thermal conductivity (mW/cm*K)	$C_x = 62$, $C_y =60$, $C_z = 76$ [4]
Two-photon absorption at 0.8μm	<0.04 cm/GW [8]

Problems with growth of the LiInS$_2$ and LiInSe$_2$ crystals were solved recently and large crystals of high optical quality became available [2, 9]. One of the typical features of ternary compounds is considerable variation of their color depending on growth or annealing conditions. Taking into account that such coloration can be due to phase transitions and affect

strongly the main output parameters including nonlinear conversion efficiency, we studied LIS and LISe samples of different color using several structurally sensitive techniques: X-ray structural analysis, nuclear magnetic resonance (NMR), frequency conversion (nonlinear susceptibility and phase-matching conditions) and optical spectroscopy and showed that color variations are due to point defects. Second harmonic generation and optical parametric oscillation were demonstrated for $LiInS_2$ for the first time.

7.2. CRYSTAL GROWTH (TASK 1)

Bulk crystals of $LiInS_2$ and $LiInSe_2$ were grown by the Bridgeman-Stockbarger (B-S) technique in the vertical set-ups with counter-pressure on seeds, prepared as rods with [001] or [010] axes direction. The ampoules with charges are moved in a thermal gradient of 10°C/cm at rate of 1-5 mm/day. This technique provides growth of crystals with diameters up to 20 mm and length up to 40 mm (Fig.1). Particular attention has been paid to purity of starting Li, In and S, Se elements. These elements were of 99.999% quality for S, Se and In, and 99.9% for Li nominal purity. Sulfur and selenium were purified by sublimation in dynamic or static vacuum, while metals were cleaned by repeated zonal melting and directed crystallization. The melt stoichiometry during growth was provided by special correction of Li/In/S (Se) ratio taking into account different ability to weight loss for these elements due to volatilization and side effect at Li interaction with the silica ampoule. To decrease the last effect synthesis was carried out in a special polished graphite crucible located inside the ampoule. The obtained crystals were transparent after growth or sometimes milky. The latter were additionally annealed in vacuum, Li_2S (Li_2Se) or S_2 (Se_2) vapor at temperature close to that of crystallizationwhich is 1000 and 900°C for $LiInS_2$ and $LiInSe_2$, respectively. Since vapor composition over the melt and partial pressure of the gaseous species are still unknown the optimized conditions for obtaining high quality crystals were found empirically. After annealing crystals become transparent but their color changes from colorless (or slight yellow) to rose one for $LiInS_2$ and from greenish to red for $LiInSe_2$.

The small variation of preparing conditions resulted to different crystal color.
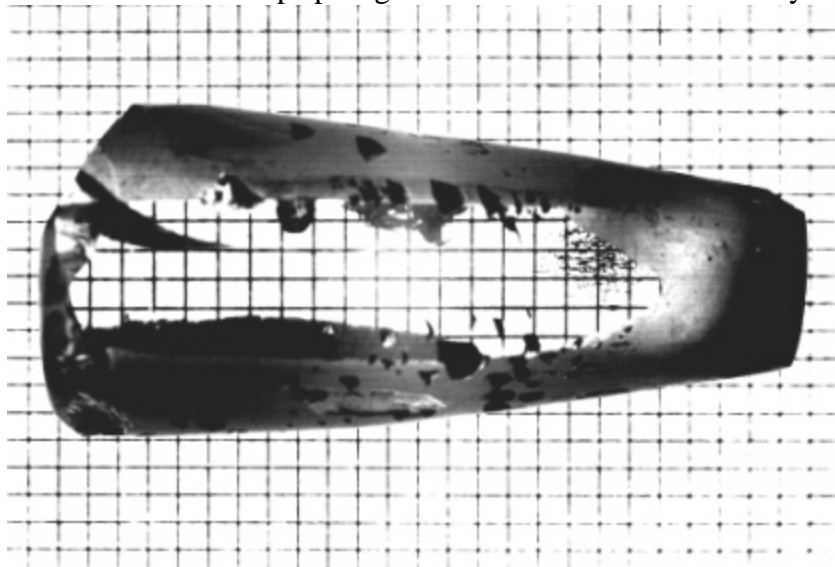
Fig.1 The $LiInS_2$ boule with two opposite polished faces, located on the net with the 2x2 mm^2 cells. Typical defects as inclusions, cracks inside boule and a number of cavities on its surface can be seen.

7.3. REAL STRUCTURE (TASK 3)

To visualize the extended defects we used different versions of optical microscopy: in transmitted or scattered light, on polished or especially etched samples, with different magnification, sometimes the polarized light was used. The usual types of extended defects are the following:

- Small, approximately isotropic inclusions, with sizes ~ 10 μm: they are responsible for milky character of as-grown crystals or of certain their parts. As in the case of other ternary chalcogenides, such as $AgGaS_2$, such inclusions bring to lower transparency of as grown crystals in the visible and near-IR region, whereas in the mid-IR their effect is much less pronounced.
- Individual lines, sometimes a lot of parallel ones, or bunches of such lines going from one point can be observed in scattered light. Our experience of investigation of other crystals using combination of optical and X-ray topography allows to suppose that these lines are due to dislocations. Their bunches are formed on large enough inclusions and are usually decorated by the small ones (Fig.2a). Sometimes a net, formed by systems of such lines directed along X or Z directions are observed: maybe such patterns are result of a domain structure (Fig.2b).
- Dendrite systems in the crystal volume (Fig. 2c): such systems were found after powerful laser processing of chalcogenide crystals.

It is necessary to note that:
1. Small inclusions distributed homogeneously in the $LiInS_2$ crystal bulk can be removed by thermal treatment in Li_2S or S_2 vapor at high enough temperatures (the same happens after annealing in Li_2Se or Se_2 for $LiInSe_2$);
2. Regarding large extended defects, which cannot be removed, they are usual only for the first stage of working out of growth technology and we have enough experience to find growth conditions for their minimizing. All mentioned types of extended defects affect considerably the wave front of the prpagating laser beam and are to be absent in nonlinear crystals.

The point defects were also studied using conventional versions of optical spectroscopy (See section 7).

Figure 2 Different types of extended defects in LiInS$_2$ and LiInSe$_2$ crystals which can be seen intransmitted or scattered light.
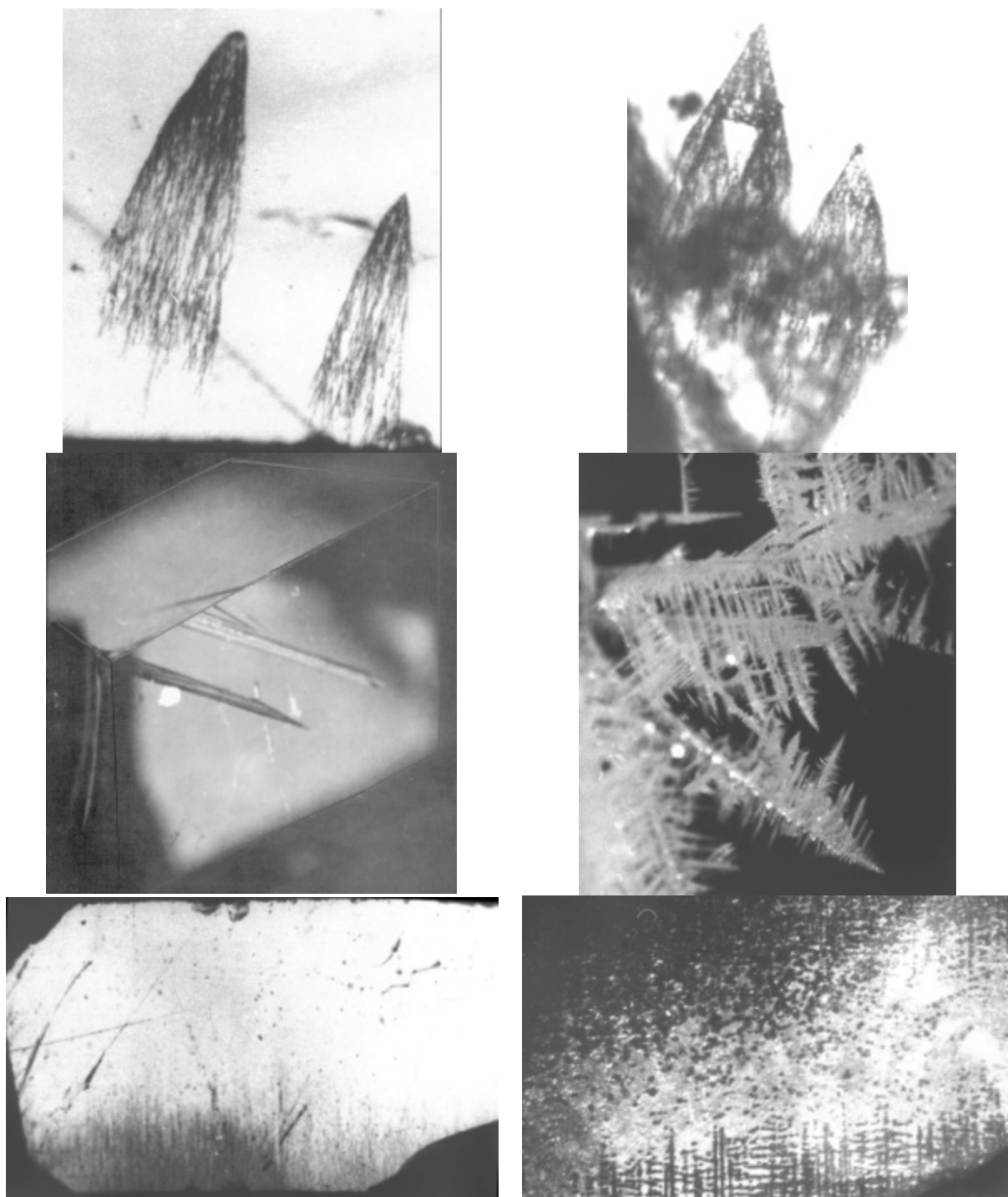
7.4. TECHNIQUES OF COMPOSITION CHARACTERIZATION AND RESULTS FOR $LiInS_2$ (TASK 1)

Total elemental analysis

The major constituents Li, In, and S, and their ratios are fixed after dissolution of 50 mG crystal in 40% aqua regia using ICP spectrometer (Perkin-Elmler ICP). Accuracy of the element determination was 3÷4 rel. %. Results of the analysis provided chemical formulae for C1-C4 samples are given in Table 2. The crystals, excluding C4, may be within the error limits assigned to almost stoichiometric ones since difference in $N_{Me}=N_{Li} + N_{In}$ to N_S ratio in real and ideal $LiInS_2$ crystals was close to zero. However, for all crystals the clear tendency to deviation from the ideal cation stoichiometry was observed because of Li deficiency and In excess.

### Table 2. Total elemental composition of the crystals C1-C4

Crystal	Composition	$N_{Li} + N_{In}$	$N_{Li+In} : N_S$	$N_{Li} : N_{In}$
C1	$Li_{0.98} In_{1.03} S_{2.32,}$	2.01	0.87	0.95
C2	$Li_{0.98} In_{1.03} S_{1.92,}$	2.01	1.03	0.95
C3	$Li_{0.96} In_{1.06} S_{1.95,}$	2.02	1.04	0.90
C4	$Li_{0.86} In_{1.04} S_{1.96,}$	1.90	0.97	0.83

3.2 Technique for determination of chemical inhomogeneity

Quantitative determination of crystal chemical inhomogeneity and analysis of inclusions are performed by differential dissolution technique. It allows local compositional analysis of bulk crystals as a function of depth to be carried out. A crystal portion of 7-15 mG is disolved layer-by-layer in a solvent flow and the solution formed enters into the detector (ICP AS spectrometer) where contents of Li, In, and S are continuously measured. Two solvents, oxidizing H_2S gas to elemental sulfur and without oxidizing, were used. It was a 40 % aqua regia at temperature about 70°C and 4M HCL at temperature as 50 °C. Since a preparation of standard references for gaseous H_2S was impossible, only relative rather than absolute values for sulfur could be determined by this technique. The metrological characteristics of the DD method are as follows: the detection limit for these elements is $10^{-2}÷10^{-3}$ µG/ml, accuracy is 3÷4 rel. %, the depth resolution is ~$2÷5·10^{-7}$ cm for the crystal with area larger than 1 cm^2. Dissolution of 15 mG $LiInS_2$ is usually takes 4÷10 min and 150÷200 composition data points are recorded for this time. The typical DD patterns involve the dissolution kinetic curves for Li, In, and S elements and lines of their molar ratios, Li/In, In/S and Li/S, taken as functions of time or of the crystal depth. The interpretation of these patterns is based on the following main concepts, which were theoretically developed and then experimentally verified on numerous examples, for instance [10-12]. A single-peaked profile of the kinetic curves corresponds to dissolution of a single–crystal. A multi-peaked profile appears for a crystal not free of grain boundaries or for a polycrystalline crystal. For a single-phase crystal the profiles of Li, In, and S kinetic curves, normalized to the maximum

dissolution rate, match exactly. The real stoichiometry of crystal dissolved is determined by the values of the lines Li/In, In/S and/or Li/S , which for an ideal $LiInS_2$ single crystal must be equal to 1, 2 and 2, respectively. In the absence of any inhomogeinety within the crystal, these ratios remain constant over the dissolution time. Departures from inearity, exceeding the error level, may be related to chemical inhomogeneity of the crystal. The location, scale, and extent of these deviations from linearity are used to determine the origin of the observed inhomogeneity. Operator experience and knowledge play a part in this interpretation.

The results obtained by the DD analysis of several portions for each of the four crystals C1-C4 were quite reproducible and typical patterns are given in Figure 3A-D. The single-peaked profile of kinetic curves and the essentially linear Li/In and S/In ratios throughout the crystal, given in Fig.3A and B, show the single crystallinity and spatial chemical homogeneity of crystals C1 and C2. The magnitudes, calculated along the whole Li/In line were found to be 0.95±0.04 for C 1 and 0.91±0.02 for C 2. These values agree well with the results of the total analysis (Table 2) that is additional evidence of the chemical homogeneity of crystals C1 and C2. Crystal C3 dissolves in a very different way (Fig.3C). The Li, In and S kinetic curves are not coincident, the Li/In and S/In lines are not entirely linear and the error values calculated over the total dissolution period are quite large, especially for S/In (Fig.3C). This means that crystal C3 is not a single crystal and spatially inhomogeneous. The gradual increase above 2 of the S/In ratio can be explained, if it is not any instrumental error, as being due to dissolution of, for instance, another kind of sulfur. A careful stepwise study of the fluctuations on these lines points out the presence of crystal areas with different Li/In and S/In values. One can suggest the dissolution of microscopic lamellae of slightly different composition and sulfur micro-precipitates located on boundaries of the lamellae. However, this idea needs further clarification. Crystal C4 obviously shows the grain structure due to milti-peaked profile of the kinetic curves and heterophase due todramatic compositional fluctuations of Li/In and S/In lines (Fig.3D). One can see that Li/In ratio keeps constant value only within the individual peaks of the kinetic curves and changes in the space between the peaks. This means that composition within the grain is identical but differs from that on the grain boundaries. With the values 0.97 and 1.98, respectively, the Li/In and S/In ratios determine the main phase as an almost stoichiometric one. Two minor phases, Li_2S (about 5 %) and elemental S (5-8 %) were detected by DD technique in C4. The Li_2S dissolves $LiInS_2$, as it can be easily seen at the beginning of the kinetic curves and Li/In and S/In lines. Sulfur, repeating the shape of the crystal, remains undissolved after completion of the main phase dissolution. So, the DD results explain the origin of nonstoichiometry determined for C4 by elemental analysis (Table 2) and demonstrate advantages of the DD analysis for obtaining reliable and correct compostion characterization of crystals.
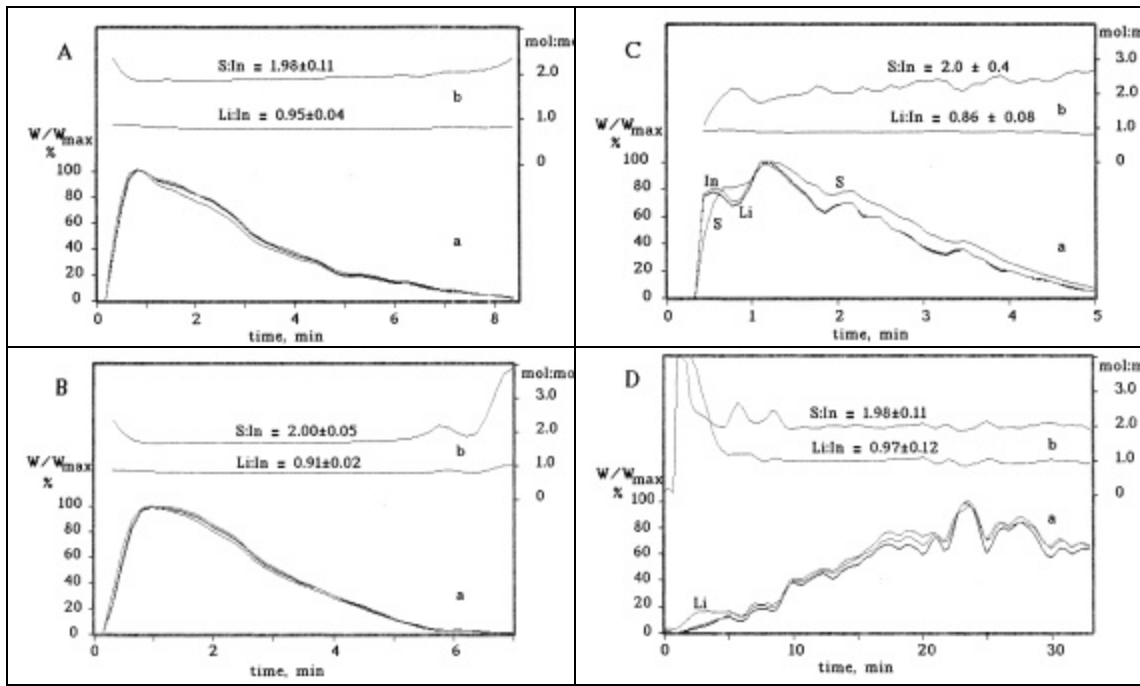
Finally, compositional characterization, performed by two different chemical methods, leads to a conclusion on obvious for C2 and C3 and possible for C1 and C4, cation nonstoichiometry being due to Li deficiency and In excess. We can discuss sulfur stoichiometry in these crystals only within the accuracy of chemical and DD analyses. Closer to stoichiometry in crystals C1-C3, native structural defect concentration is reduced and stoichiometric C1 dissolves as a single crystal without oscillations on Li/In and S/In lines, slightly nonstoichiometric C2 has minor oscillations on the lines. Crystals C3 and C4 crumble during dissolution instead of dissolving layer-by-layer, as it is observed for single crystal C1 and C2 and show visible oscillations on the lines. Besides, under equal conditions the dissolution time of crystals C1, C2 and C3, weighting 7.0, 7.1 and 11.2 mG, respectively, reduces from 8 to 5 minutes in accordance with increase of their disorder (Fig.3A-C). The quite slow dissolution of C4 (Fig.3D) can be explained as being due to location of sulfur on the grain boundaries, which delay dissolution of the $LiInS_2$ matrix.

Thus the as-grown samples are almost colorless for LIS or yellow to greenish for LISe. For as-grown samples chemical analysis indicates 1 to 3% deficit of chalcogen relative to metals (Li+In), on the other hand there is 2 to 4% Li deficit relative to In [2]. There is a lot of small inclusions inside as-grown LIS and LISe crystals which make them milky and one uses a high temperature annealing in chalcogen vapor to make samples highly transparent. It is the widespread technological treatment, which is used for other crystals such as $AgGaS_2$ or $AgGaSe_2$. Indeed, chemical analysis shows up to 3% surplus S or Se [2] after annealing, but in contrast to the mentioned compounds, LIS and LISe change their color considerably after annealing: Annealed LIS is rose and LISe becomes dark red to opaque. Since the phase diagram can be very complicated for ternary compounds and the area of homogeneity related to a certain phase is sometimes only about 1 wt.% in width, it is necessary to verify that the crystal structure remains unchanged after annealing. Thus, as-grown and annealed samples of LIS and LISe were compared using different structurally sensitive techniques: X-ray structural analysis, nuclear magnetic resonance, optical spectroscopy, refractive indices, nonlinear frequency conversion et al.

7.5. THE X-RAY STRUCTURAL ANALYSIS (TASK 2)

The crystal structure determination for different LIS and LISe samples was performed using CAD4 diffractometer along with the SHELXL97 structure determination/refinement program. For all samples investigated identical structure (space group $Pna2_1$, wurtzite- type lattice) was established, but lattice parameters somewhat varied: they increased in line with color intensity (Table 3).

Table 3. Lattice parameters for $LiInS_2$ and $LiInSe_2$ single crystals of different color determined in the present work in comparison with Ref. [1,13]

Crystal	$LiInS_2$			$LiInSe_2$			
Color	Colorless,C1	Yellowish,C2	Rose, C3	Yellow	Greenish	Rose	Dark red
Space group	$Pna2_1$	$Pna2_1$	$Pna2_1$	$Pna2_1$	$Pna2_1$	$Pna2_1$	$Pna2_1$
a [⊕]	6.874(1) 6.894 [1]	6.890(1)	6.896(1)	7.1917(8)	7.192	7.1939(8)	7.1934(10) 7.218 [13]
b [⊕]	8.0332) 8.064 [1]	8.053(1)	8.058(2)	8.4116(10)	8.412	8.4163(10)	8.4159(11) 8.441 [13]
c [⊕]	6.462(1) 6.485 [1]	6.478(2)	6.484(4)	6.7926(8)	6.793	6.7926(8)	6.7971(9) 6.772 [4]
V [⊕^{3}]	356.82 360.5 [1]	359,43	360.3	410.90(8)	410.97	411.27(8)	411.49(9) 412.6 [13]

7.6. NUCLEAR MAGNETIC RESONANCE: $LiInSe_2$ (TASK 2)

Both ^7Li ($I=3/2$) and ^{115}In ($I=9/2$) are quadruple nuclei: their NMR line shape is sensitive to the variations of the structure of compound and to existing defects. Single crystals of LISe 3.5 x 3.5 x 5 mm^3 in size were placed into a NMR coil of 5 mm in diameter. The powder samples were prepared also from the same crystals. The ^7Li and ^{115}In spectra were measured with a Tecmag pulse NMR spectrometer in the applied magnetic field of 8.0196 T (at resonance frequencies 132.68 and 74.84 MHz for ^7Li and ^{115}In nuclei, respectively), using Fourier transformation of the spin echo signals accumulated with the 16-phase cycled sequence. The length of p/2 pulse was 4 µs for ^7Li and 5 µs for ^{115}In. Angular dependence was measured when the crystals were rotated around their *c*-axis, which was perpendicular to the applied magnetic field. All samples exhibited very long spin-lattice relaxation time (around 1 *h*) which is characteristic for high purity compounds.

^7Li and ^{115}In NMR spectra of LISe single crystals and powders are given in Fig. 4A and Figs. 4B-4C, respectively. Both ^7Li and ^{115}In should show quadrupolar perturbed NMR signals. In single crystal, the NMR spectrum of ^7Li nucleus with $I=3/2$ consists of three lines. Besides a single resonance at Larmor frequency $?_0$, two satellites with the first-order shift of

$$? _1=e^2qQ(3\cos^2? -1)/4h \qquad (1)$$

occur. Here *q* is the electric field gradient (EFG), *Q* is the quadruple moment of the nucleus, ? is the angle between applied magnetic field and the principal axis of the EFG tensor, and *h* is the Planck's constant. The aforementioned satellites are clearly seen in the ^7Li spectrum of single crystal (Fig. 4A). In the powder (Fig.4B), the central line and the satellites are almost

unresolved due to the overlap caused by angular dependence of the resonance frequency given by Eq. (1). For [115]In nucleus with $I=9/2$, nine satellites should occur. However, they are hardly excited with our p /2 pulse, and thus we show
and analyze only the central line corresponding to ?? -? transition.
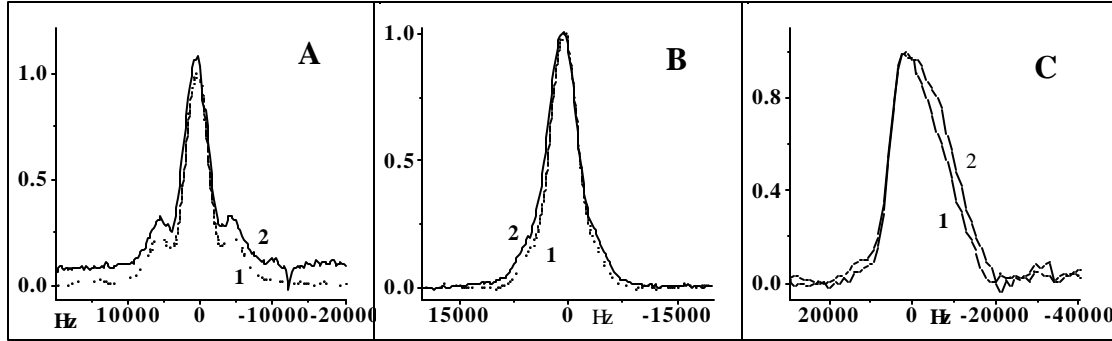
**Fig. 4: A.** Room temperature ^{7}Li NMR spectra of single crystal $LiInSe_2$ corresponding to the maximal splitting of the lines. Orientation of external magnetic field B_0 is: B_0- **c**, angles (B_0, **a**)=22.5°, (B_0, **b**)=67.5° (with accuracy about 2-3°). For as-grown (1) and annealed (2) samples, the spectrum of the latter is shifted upwards for clarity. **B** and **C:** Room temperature ^{7}Li and [115]In NMR spectra for as-grown (1) and annealed (2) powder $LiInSe_2$, respectively.

Line width of the quadrupolar perturbed NMR signals are caused by dipole-dipole interaction of nuclei and distribution of electric field gradients existing in an imperfect crystal. The nearest neighbors of In and Li atoms are Se atoms. Due to the low natural abundance of [77]Se isotope (7.6%) having nuclear spin and rather large Li-Li, In-In and Li-In distances (around 4.1 ?), the dipole-dipole interactions among nuclei are weak; their contribution into the second moment of the resonance line is calculated to be around 1 kHz^2 for both [7]Li and [115]In. Moreover, the dipole-dipole interactions should be the same for the as-grown and annealed samples. Thus the main contribution to the line width results from the distribution of EFGs, and the difference in the line width is caused by the variation of this distribution in annealing. From Fig. 1B-C, one can see that the powder ^{7}Li and [115]In NMR spectra of as-grown and annealed LISe are very similar, though the resonance of the annealed sample is a little bit broader. Two reasons are suggested:

1. The EFG distributions on Li and In nuclei are broader in the annealed sample, which is less perfect than the as-grown one. It may be, for example, because surplus Se atoms occupy the unfilled tetra- or octahedral sites of the lattice. Such an imperfection of the crystal creates an additional electric field gradient at nucleus; these gradients vary from site to site and yield additional line broadening.

2. The structural parameters of the two samples are a little bit different, resulting in EFG values larger in the annealed sample than in the as-grown one. Such effect would lead to a difference in the quadruple splitting of the NMR spectra of the two crystals, which is not obtained in the single crystalline spectra (Fig.4A). Thus one can conclude that both as-grown and annealed $LiInSe_2$ samples have identical crystal structure and the negligible differences in NMR spectra can be related to point defects such as surplus Se ions in different positions in crystal lattice.

7.7. OPTICAL ABSORPTION SPECTROSCOPY (TASK 2,3)

Optical transmission spectra in the whole transparency region were recorded, using Shimadzu UV-3101 PC UV/VIS-NIR and Bomem FTIR spectrometers. Both shortwave and longwave edges
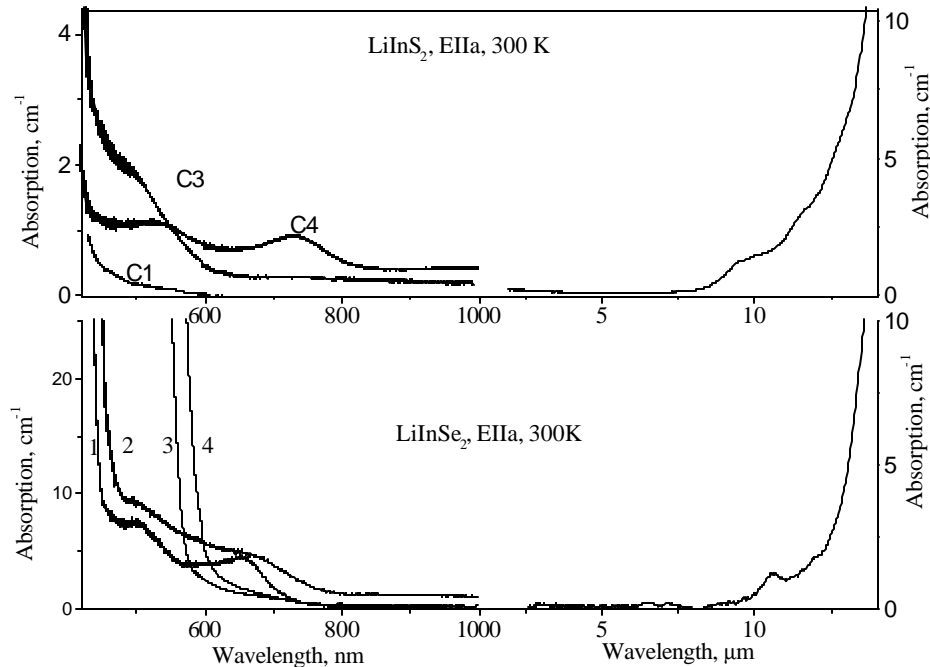
Fig.5 Absorption spectra for LIS (A) and LISe (B) samples. In A: C1 and C4 are as-grown LIS samples while C3 was annealed [2]. In B spectra 1,2 were obtained for yellow as grown LISe and 3,4 correspond to a dark red sample. Spectra 1,3 and 2,4 were recorded at 80 K and 300 K, respectively.

of the transparency region are important for crystal characterization. The latter is determined by lattice vibrations and one can see in Fig.5 that both for LIS and LISe it is identical in shape and position for as-grown and annealed crystals. The shortwave absorption edge characterizes band-to-band electronic transitions: in real crystals the near-edge absorption bands due to native defects mask it usually and this is the reason why thin samples, less than 0.1 mm thick are studied. For LIS this work was reported in [2]. In both as-grown colorless and annealed rose samples the absorption spectra were found to become straight lines in $(a^*h?)^2 = f (h?)$ coordinates and to lead to identical band gap values: E_g= 3.72 and 3.59 eV at 80 and 300K, respectively. The rose color of thick annealed LIS samples was due to broad bands at 420 and 540 nm [2]. For as-grown LISe the same approach gave E_g=3.04 and 2.86 eV at 80 and 300K [14], respectively, but for annealed samples some additional intense bands with maxima in the 500 to 550 nm range superimpose the fundamental edge even at 0.1 mm thickness and it was necessary to decrease the thickness further. As a result annealed thin plate is red in color. It is important to note that illumination by a visible light with ?~400-500 nm from 1kW Xe lamp through MDR2 diffraction monochromator was found to remove the red color of annealed $LiInSe_2$ crystals and to make them yellow, the effect being reversible. Such effects are typical of the recharge of point defects in solids.

7.8. REFRACTIVE INDICES (TASK 4)

LiInS$_2$: Refractive indices for LiInS$_2$ were measured using the conventional technique of minimum deviation angle in [1]. The theoretical curve for phase-matching conditions was built using the refractive indices from [1] and fitting equation as

$$n^2 = A + B/(C + ?^2) + D?^2 \quad (2)$$

with A, B, C, D, values from Table 4 [15]

Table 4. Sellmeier parameters for LiInS$_2$ [15].

	a or Y	ß or X	? or Z or 2 fold axis
A	4.418222	4.559534	4.59206
B	0.1254461	0.1403701	0.1410887
C	-0.0657432	-0.069233	-0.069287
D	-0.0028850	-0.0028731	-0.0030589

LiInSe$_2$: The refractive index of yellow LiInSe$_2$ was measured using two prisms with different orientation and edges of ~ 6 mm by the same technique. The results are presented in Table 5. The principal values n_z and n_y appear to be very close and the convention $n_x < n_y < n_z$ leads to the correspondence *abc=yxz* between the crystallographic and the principal optical axes. The principal values of refractive indices were fitted by Sellmeier equations of the same type as known for LiInS$_2$ (See **[2]):** with coefficients given in Table 6. Also given in the Table are the maximum deviations ? from the measured index values. LiInSe$_2$ is a negative biaxial crystal with an angle between the two optic axes of $2V_z=140°$ at 532 nm (137° for LiInS$_2$ in Ref.[16]). According to the Sellmeier equations LiInSe$_2$ is phase-matchable for SHG at 10.6 µm only in the *x-z* plane with type-I (oo-e) interaction.

To compare the refractive indices of LiInSe$_2$ of different color we measured these parameters for one and the same LiInSe$_2$ prism before and after annealing in Se$_2$ vapor: the prism was yellow before annealing and became red after the treatment (Table 7). One can see that refractive indices are identical within the experiment accuracy.

Table 5. Refractive indices versus wavelength for LiInSe$_2$ (abc=yxz)

Wavelength [μm]	$n_a=n_y$	$n_b=n_x$	$n_c=n_z$
0.5	-	2.5228	2.6035
0.525	-	2.4849	2.5594
0.55	2.5178	2.4549	2.5248
0.575	-	2.4313	2.4977
0.600	-	2.4118	2.4758
0.650	2.4331	2.3818	2.4422
0.700	2.4079	2.3601	2.4174
0.750	2.3893	2.3436	2.3989
0.800	2.3746	2.3306	2.3843
0.850	-	2.3196	2.3725
0.900	2.3533	2.3109	2.3632
0.950	-	2.3037	2.3550
1.000	2.3390	2.2977	2.3486
2.000	2.2913	2.2530	2.2988
3.000	2.2842	2.2434	2.2891
4.100	2.2799	2.2398	2.2842
5.000	2.2772	2.2370	2.2818
6.000	2.2718	2.2323	2.2765
7.000	2.2688	2.2271	2.2715
8.000	2.2612	2.2202	2.2649
10.000	2.2522	2.2015	2.2566
11.000	2.2352	2.1935	2.2380

Table 6. Sellmeier coefficients A, B, C, D for LiInSe$_2$ and maximum deviation of the fit ?.

	a or Y	ß or X	? or Z or 2 fold axis
A	5.2026545	5.0370599	5.2399142
B	0.242247	0.2165833	0.2414178
C	0.0899151	0.0856929	0.091789
D	0.0015069	0.0018534	0.0017645
?	0.00585	0.00264	0.00585

Table 7. Comparison of refractive indices for LiInSe$_2$

?, nm	Yellow-greenish LiInSe$_2$		Dark red LiInSe$_2$	
	n_x	n_z	n_x	n_z
700	2.3627	2.4215	2.3615	2.4219
800	2.3341	2.3886	2.3347	2.3752
900	2.3130	2.3656	2.3138	2.3662
1000	2.3004	2.3507	2.3006	2.3513
1500	2.2704	2.3188	2.2709	2.3186

| 1900 | 2.2619 | 2.3082 | 2.2619 | 2.3090 |

## 7.9. NONLINEAR THREE-WAVE INTERACTION

LiInS$_2$: Second Harmonic Generation (SHG) and Optical Parametric Oscillation(OPO)

Optical elements from LiInS$_2$ single crystals of different color were cut for type-II phase-matching in the XY (eoe interaction) and YZ (oeo interaction) planes. The effective nonlinearity is given by:

$$d_{eff}^{XY} (f, ? =90) = d_{32} \sin^2 f + d_{31} \cos^2 f \qquad (3)$$

$$d_{eff}^{YZ} (f =90 , ?) = d_{32} \sin ?. \qquad (4)$$

The correspondence between the crystallographic and the dielectric axes chosen is a,b,c=Y,X,Z. Two laser sources were used in the SHG experiments: (1) picosecond pulses from the free-electron laser (FEL) for infrared experiments (FELIX, the Netherlands) [17] in the wavelength range 2.75-6.0 µm and (2) a nanosecond OPO tunable near 2.5 µm. A 'yellow' sample of 3x2 mm^2 aperture and a 'rose' sample of 5x3 mm^2 aperture, both 2 mm in length and cut at ? =90° and f=55°, were used for short pulse SHG experiments on the FELIX set-up. Several samples of equal aperture (4x4 mm^2) and length between 5 and 7 mm cut at f =66-66.6 , ?=90 (XY plane) and ?=28 , f=90 (YZ plane) were used for SHG experiments with nanosecond pulses. The measurements showed +3° difference as compared to calculation based on the refractive index data [1] near 2.5 µm for interaction in the XY plane and larger deviations, up to +6º, in the YZ plane [7]. The discrepancy increased at longer wavelengths approaching -10º in the XY plane at 6 µm. Only slight difference could be observed between yellow and rose samples, shown in Fig.6 by open and solid dots, respectively.
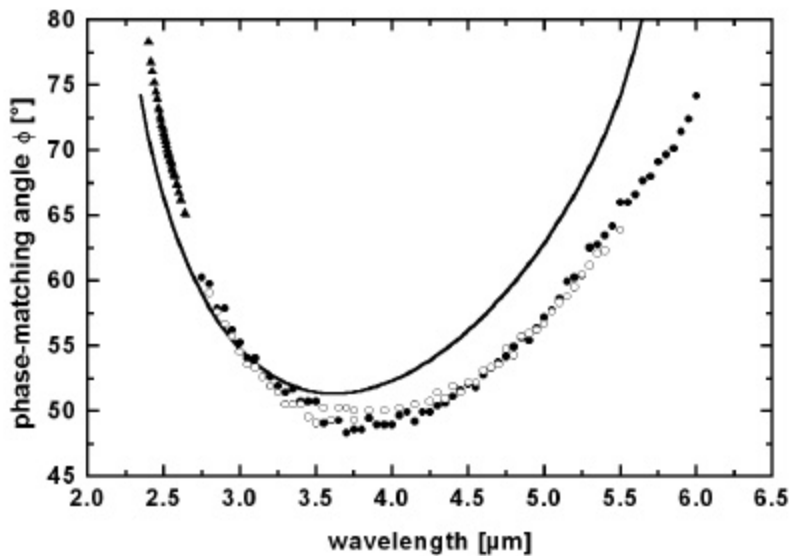

Figure 6. Second harmonic generation in the XY plane: Measured internal phase-matching angles for the 'rose' (solid dots) and 'yellow' (open dots) LiInS$_2$ crystals. The line is the calculated phase-

matching curve based on the refractive index data from [1]. The solid triangles are measurements performed with a similar 'rose' LiInS$_2$ crystal, using a nanosecond OPO as a pump source.

A KTP crystal, type –II (oeo) phase-matched for the same SHG (?= 56.6 , f=0°) in the XZ plane was used as a reference sample where d$_{eff}$(KTP)= d$_{32}$ sin ? = 2.3 pm/V. For yellow and rose samples tensor components of d$_{31}$ =8.35 pm/V and d$_{32}$ =8.3 pm/V were deduced both from precise gaussian beam analysis of the SHG process and also by relative measurements. These values are only slightly lower than estimations based on non-phase matched methods presented in [1] at 10.6 µm (d$_{31}$ =9.9 pm/V and d$_{32}$ =8.6 pm/V). Thus, phase-matching conditions and nonlinear susceptibility are similar for yellow and rose samples, which confirms the conclusion about the identity of their structure.

Most of the existing mid-IR femtosecond laser sources are based on frequency conversion in nonlinear crystals using the widely spread and reliable Ti:sapphire lasers/amplifiers that are tunable near 800 nm. That is why search for new nonlinear crystals for producing idler wavelengths in the mid-IR without two-photon absorption for 800 nm pumping is of great importance.

We presented in [8] initial results with an uncoated 1.5-mm-thick LiInS$_2$ sample cut at f=41°, ?=90° and used as a traveling wave optical parametric amplifier for pumping with a tunable 1 kHz femtosecond Ti:sapphire regenerative amplifier. Here we report an improvement by a factor of about 50 for the output idler energy using a rose sample of the same cut and a length equal to 5 mm. For tuning we used five interference filters between 875 and 975 nm to select a ˜ 10 nm portion of the continuum generated using the same pump source in a 2-mm thick sapphire plate at the signal wave. The output idler and the input seed (signal) energies as well as the internal signal gain achieved are presented versus idler wavelength in Fig.7. One can see that such a femtosecond optical parametric amplifier covers the 5 to 12 µm spectral range where the pulse duration (<600 fs) corresponds to almost bandwidth-limited idler pulses. From 8 to 12 µm we achieved almost constant energy level of >80 nJ for the idler (it is lower at <8 µm). The high parametric gain at wavelengths where LiInS$_2$ already absorbs can be explained by the advantageous (lower) mismatch between the three group velocities [8].
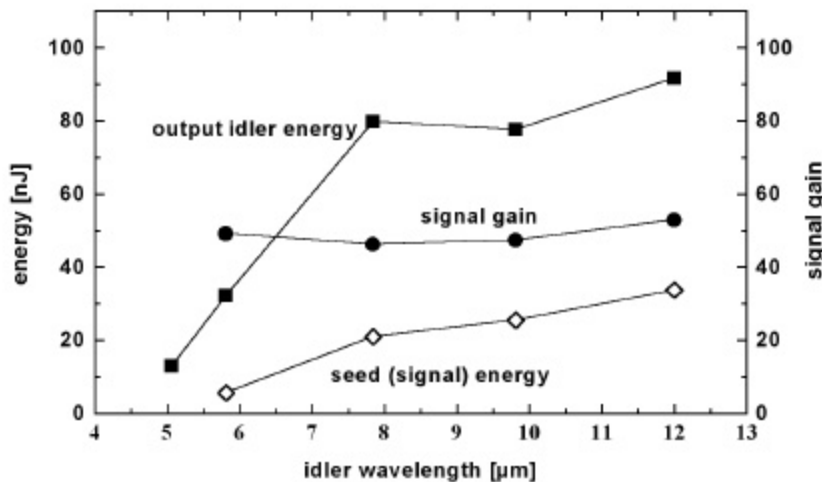
Fig.7 Optical parametric amplification in LiInS$_2$: signal gain, output idler energy and seed (signal) energy versus idler wavelength. The pump wavelength is 820 nm, and the peak pump intensity amounts to 60 GW/cm^2 using 150 µJ, 300 fs pump pulses.

Conclusions

- Combined investigation of as-grown and annealed, colored $LiInS_2$ and $LiInSe_2$ crystals using X-ray structural analysis, NMR, optical absorption spectroscopy, refractive indices and phase matching conditions showed identity of their structure and of their main physical properties, which allows to associate the coloration at annealing in chalcogen vapor with point defects.
- The nonlinear coefficients of $LiInSe_2$ and $AgGaS_2$ are comparable and it is clear that for some combinations of wavelengths and polarizations $LiInSe_2$ will have larger effective nonlinearity. The *mm2* symmetry of the latter offers possibility for noncritical II type interaction for any pump wavelength, the limits being set only by the transparency window of the crystal. In particular, pumping of noncritical configuration near 1 **µ**m is possible. In uniaxial crystals with chalcopyrite structure ($AgGaS_2$ et al.) the *42m* symmetry leads to vanishing effective nonlinearity in the 90º limit of noncritical type II interaction.
- **Taking into account such advantages as high thermal conductivity, large energy gaps, low two-phonon absorption, high damage threshold we suggest this crystal as promising new material for second-order nonlinear frequency conversion in the mid-IR.**

References

1. G. D. Boyd, H. M. Kasper, and J. H. McFee, J. Appl. Phys. **44**, 2809-2814 (1973).
2. L. Isaenko, I. Vasilyeva, A. Yelisseyev, S. Lobanov, V. Malakhov, L. Dovlitova , J.-J. Zondy, I. Kavun, J. Cryst. Growth, **218**, 313-321 (2000).
3. J.Mangin, S. Salaün, S.Fossier, P. Strimer , J.-J. Zondy, L. Isaenko, A.Yelisseyev, Optical properties of lithium thioindate. Proc. Photonics West-2001, Proc.SPIE v.**4268** (2001) 45-57.
4. C.Ebbers , LLNL, USA, private communication.
5. T.Kamijo, K.Kuryama, Single crystal growth of $LiInS_2$, J.Cryst.Growth, **46**/6 (1979) 801-3;
6. TK Negran, HM Kasper AM Glass, Pyroelectric and electrooptic effects in $LiInS_2$ Mat.Res.Bull 8/6 (1973) 743-6;
7. GMH Knippels, AFG van der Meer, AM MacLeod. A.Yelisseyev, L.Isaenko, S.Lobanov, I.Thenot, J.-J.Zondy, Mid-infrared (2.75-6.0 µm) second harmonic generation in $LiInS_2$, Opt.Letters 26/9 (2001) 617-9;
8. F.Rotermund, V.Petrov, F.Noack, L.Isaenko, A.Yelisseyev, S.Lobanov, Optical parametric generation of femtosecond pulses up to 9 µm with $LiInS_2$ pumped at 800 nm, Appl.Phys.Letters, 78/8 (2001) 2623-5;
9. L. Isaenko, A. Yelisseyev, S. Lobanov, F. Rotermund, V. Petrov, G. Slekys, and J.-J. Zondy, A new ternary chalcogenide crystal for nonlinear optical application in the mid-IR: $LiInSe_2$, J. Appl. Phys. (2001), in press.
10. VV Malakhov, Zh. Analit. Khim.*,* **49** (1994) 349.
11. IG Vasilyeva, VV Malakhov, A .A. Vlasov, and MR Predtechensky, Thin Solid Films   **292** (1997) 85.
12. IG Vasilyeva, VV Malakhov, LS Dovlitova and H Bach, Mater. Res. Bull. **34** (1999)81.

13. T. Kamijoh and K. Kuriyama, J. Cryst. Growth **51**(1981) 6-11 .
14. L. Isaenko, A. Yelisseyev, J.-J. Zondy, G. Knippels, I. Thenot, S. Lobanov, Opto-electronic review, **9**, 135-141 (2001).
15. Ch.Ebbers, "Summary of known nonlinear properties of $LiInS_2$", preprint **UCRL-ID-116744** Feb. 1994, LLNL, Livermore, USA.
16. A.Yelisseyev, L. Isaenko, S. Lobanov, J.-J. Zondy, A. Douillet, I. Thenot, Ph. Kupecek,G. Mennerat, J. Mangin, S. Fossier, and S. Salaün, New ternary sulfide for double applications in laser schemes, in Advanced Solid State Lasers, H. Injeyan, U. Keller and C. Marshall, eds. Vol.34 of OSA Trends in Optics and Photonics Series (Optical Society of America, Washington, D.C., 2000), pp.561-568.
17. GMH Knippels, X.Yan, AM MacLeod, WA Gillespie, M Yasumoto, D Oepts, AFG van der Meer, Generation and complete electric-field characterisation of intense ultrashort far-infrared laser pulses, Phys.Rev. Letters 83/8 (1999) 1578-81.

All tasks 1-4 have been done according Scope of Activity. Obtaining results demonstrate that $LiInS_2$ and LiInSe2 are promising new materials for nonlinear application

Optical elements were delivered to Partner according Schedule:

10.05.2001. 9 polished plates 6x6x1 mm^3 in size from $LiInS_2$ with short edge, parallel to X, Y, Z (3 plates of each type for three groups of measurements: residual absorption, electrical measurements, deep level spectroscopy);

06.08.2001. 2 prisms from $LiInS_2$ with different orientation and 30^0 apex angle for refractive index measurements for three polarizations;

14.11.2001. 9 polished plates 6x6x1 mm^3 in size from $LiInSe_2$ with short edge, parallel to X, Y, Z (3 plates of each type for three groups of measurements: residual absorption, electrical measurements, deep level spectroscopy);

19.12.2001. 2 prisms from $LiInSe_2$ with different orientation and 30° apex angle for refractive index measurements for three polarizations;

The reports with sample description have been forwarded in line with optical elements delivery beginning from Quarter 1 to Quarter 4. A paper and a report have been submitted, participation in the MRS conference took place in November 2001 in the U.S.A.

According Technical Schedule Isaenko L.I. took part in MRS 2001 Fall Meeting in Boston, November 26-30, 2001 with Report "CHARACTERIZATION OF $LiInS_2$ AND $LiInSe_2$ SINGLE CRYSTALS FOR NONLINEAR APPLICATIONS". Ludmila Isaenko, Alexander Yelisseyev, S. Lobanov, V. Vedenyapin, (Russia, DTIM), A.Panich, Ben-Gurion (University of the Negev, Israel), J-J Zondy (Observatory of Paris, France), V.Petrov (MB-Institute, Germany), G.Knippels (FOM-Institute for Plasma Physics, Netherlands). The paper was submitted for publication in Proceedings of MRS.

8. Technical Schedule

	1 Quarter	2 Quarter	3 Quarter	4 Quarter	**TOTAL Task effort** **Man*mths.)**
Task 1	$LiInS_2$		$LiInSe_2$		
Estimated Effort (man*mths.)	2.9	2.8	2.8	2.8	11.3
Task 2	$LiInS_2$		$LiInSe_2$		
Estimated Effort (man*mths.)	3.0	2.6	2.6	2.6	10.8
Task 3	Supply of 9 $LiInS_2$ plates	Supply of 2 $LiInSe_2$ prisms	Supply of 9 $LiInS_2$ plates	Supply of 2 $LiInSe_2$ prisms	
Estimated Effort (man*mths.)	2.0	2.0	2.0	2.0	8.0
Task 4		Report, presentation of publication	Report at Conference	Final report	
Estimated Effort (man*mths.)		0.5	0.5	0.5	1.5
TOTALQuarter effort Man*mths.)	7.9	7.9	7.9	7.9	31.6

Attachment 1

9.1 Individual participants

Category 1 (Weapon Scientific and Technical Personnel)

Name	Birth Year	Scientific Title	Weapon Expertise Ref.	Function in project	Daily rate (US$)	Total days	Total g (US$
1. Isaenko Ludmila	1946	Prof.	1.2. Techniques	Manager of project	35	220	770
2. Yelisseyev Alexander.	1947	Dr.	for guidance	Investigation of physical parameters	32	191	61
3. Lobanov Sergey.	1953		and control of missiles	Crystal growth	25	168	420
				Total:		**579**	**180**

9.2 Managerial responsibilities

Director of DTIM SB RAS (Chepurov Anatoly)
↓
Project Manager (Head of Lab Isaenko Ludmila)
↓
Participants of Project (Yeliseyev Alexander, Lobanov Sergey)

10. Table for Materials Summary

TABLE 3

EQUIPMENT/MATERIAL SUMMARY					

MATERIAL SUMMARY

for Project Agreement # 2006P

To be provided in kind [..]

To be purchased by Design & Techlogical Institute of Monocrystals SB RAS [+]

The ISTC will normally provide the most appropriate equipment that will perform the functions required; however, if very special reasons are given and explained in detail (Form PR-2E), the purchase of a particular make will be considered.

Item No.	DESCRIPTION OF ITEM Please list items in the order of their priority and put an 'X' in the column next to "Item no." if ISTC form PR-2E, "Data for a Single Equipment Item', has been completed for a given item and is attached.		Date Needed (quarter)	Qnt., g	Unit cost (in USD)	Amount (in USD)
1.Name of Institution:		**Design & Technological Institute of Monocrystals SB RAS**				
1.		Indium (metal)	I quart.	400	1.50	600.00
2.		Sulphur	I quart.	408	1.25	510.00
3.		Selenium	I quart.	400	1.63	652.00
Subtotal						**1,762.00**
2.Name of Institution:						
Subtotal						
Estimated TOTAL COST						**1,762.00**

Form PR-1M from 3/98

Budget expenditure was related to Financial plan

Project Manager Isaenko Ludmila Ivanovna